EPiC Series in Technology
Volume 4, 2026, Pages 75–82
Proceedings of The 11th International Conference on Tribology in Manufacturing Processes & Advanced Surface Engineering

Effect of Clearance on Punching-Hole Surface Crack Width in the Shearing of Amorphous Electrical Steel Sheets Using a Tool with a Nanometer-Scale Periodic Structure

Tomomi Shiratori[1], Nanaka Takahashi[2], Mitsuaki Ikeda[2] and Tatsuhiko Aizawa[3]
[1] Faculty of engineering, University of Toyama, Japan.
[2] Graduate school of Engineering, University of Toyama, Japan.
[3] Surface Engineering Design lab., Tokyo, Japan.
shira@eng.u-toyama.ac.jp, m25c1449@ems.u-toyama.ac.jp,
s2270408@ems.u-toyama.ac.jp, taizawa@shibaura-it.ac.jp

Abstract

Amorphous electrical steel sheets were sheared using a tungsten carbide–cobalt (WC–Co) punch. To suppress crack initiation on the pierced-hole surface, the punch was first subjected to ion sharpening and subsequently laser processed to introduce a nanometer-scale periodic structure. The shearing characteristics were compared with clearance as a parameter. The fracture propagation mechanism was analyzed based on the crack behavior and the load–stroke diagrams. The results showed that the introduction of the nanometer-scale periodic structure and the reduction of the clearance to as small as 1 µm successfully suppressed crack formation, and that clearance is the dominant factor in crack inhibition.

1 Introduction

The improvement of motor efficiency is regarded as a key technology supporting an electrified society [1]. Amorphous electrical steel sheets, which exhibit excellent magnetic properties such as low iron loss and high magnetic permeability, have attracted considerable attention as core materials for high-efficiency motors [2–4]. It has been reported that their efficiency is further enhanced under high-frequency operating conditions [5–7]. Numerous studies on the shearing of amorphous electrical steel sheets have been reported [8–10]. However, these materials show a high tensile strength of approximately 2.2 GPa and a limited elongation of about 1%, resulting in brittle fracture behavior. In addition, their high hardness, exceeding 900 HV, leads to rapid tool wear during shearing.

A laminated shearing process has been proposed [11]. Nevertheless, controlling brittle fracture behavior remains difficult. As a countermeasure against tool wear, it has been reported that applying a 10 µm chamfer to the punch edge reduces tool wear to less than 5 µm even after 50,000 punching cycles [11]. Cracks formed on the pierced-hole surface increase iron loss; therefore, the development of a shearing technique capable of suppressing crack formation is strongly required. A sharp cutting edge is effective for crack suppression, and ion-sharpening technology has been proposed for this purpose [12]. When applied to the punching of stainless steel, the affected zone on the pierced cross-section is reduced. Furthermore, tools with nanometer-scale periodic groove structures fabricated on the tool surface by laser processing have been developed. When such tools are applied to the shearing of non-oriented electrical steel sheets, the work-hardened region on the pierced cross-section is restricted [13,14]. In addition, extensive studies have been conducted on the application of nanometer-scale periodic surface structures to the shearing of amorphous electrical steel sheets [15–18]. However, in these studies the clearance was relatively large—approximately 5 µm for a sheet thickness of 25 µm (25% of the sheet thickness)—and complete suppression of cracking on the pierced-hole surface has not yet been achieved.

In the present study, amorphous electrical steel sheets were sheared under an ultra-small clearance of 2 µm or less, corresponding to less than 10% of the sheet thickness, using both a conventionally polished tool and a tool subjected to ion sharpening followed by the introduction of a nanometer-scale periodic surface structure. The objective of this study is to clarify the crack formation behavior on the pierced-hole surface under narrow-clearance conditions and to elucidate the mechanism of crack suppression.

2 Experimental Procedure

In this experiment, a servo-driven screw press machine (DT-J311, Micro Processing Laboratory Co., Ltd.; maximum load capacity: 10 kN) was used in experiments. An AISI D2(JIS SKD11) die set was employed as the piercing experiments. A load cell (LBMT-A-500N, Kyowa Electronic Instruments Co., Ltd.) was mounted on the die to measure the piercing load, while the stroke was measured using a spectroscopic confocal laser displacement sensor (LK-G30, KEYENCE Co., Ltd.). The load and stroke data were acquired using a data logger (NR-600, KEYENCE Co., Ltd.). All measured data were transferred to a personal computer via an interface for subsequent analysis.

The workpiece material was a single amorphous steel sheet with a thickness of 25 µm and a material composition of Fe–3Si (Metglas 2605HB, Proterial, Co., Ltd.). The maximum load of the servo press system was set to 30 kN. All experiments were conducted under unlubricated dry conditions, and the punching speed was set at 5.0 mm/s.

The conditions of the punches and dies used in this study are summarized in **Table 1**, and SEM images of their cutting edges are shown in **Figure 1**. As the punch material, cemented carbide was used, and two types of punches were prepared: a conventionally ground punch and a punch subjected to ion sharpening followed by the introduction of a nanometer-scale periodic structure with diamond like coating (DLC). For the die, both a conventional ground condition and an ion-sharpened condition were also prepared. The clearance was set to 5 µm as the standard condition. For the tool with the nanometer-scale periodic structure with DLC, additional clearances of 2 µm and 1 µm were employed.

Load–stroke diagrams were calculated from measurement data, and the crack width on the surface of the piercing holes were measured using a scanning electron microscope (SEM) (JCM-700, JEOL Ltd.). The front, back, left and right sides of the punched hole surface were observed by SEM.

Condition	Clearance [μm]	Punch		Die	
		Finishing	Outer diameter [mm]	Finishing	Inner diameter [mm]
Normal	6.0	Ground	4.992	Ground	5.004
Ion+Nano+DLC	5.5	Ion Polish, Nano-texturing, DLC	4.999	Ion Polish, Nano-texturing, DLC	5.010
Ion+Nano+DLC	2.0	Ion Polish, Nano-texturing, DLC	4.998	Ion Polish, Nano-texturing, DLC	5.002
Ion+Nano+DLC	1.0	Ion Polish, Nano-texturing, DLC	4.998	Ion Polish, Nano-texturing, DLC	5.000

Table 1: Punch and die conditions

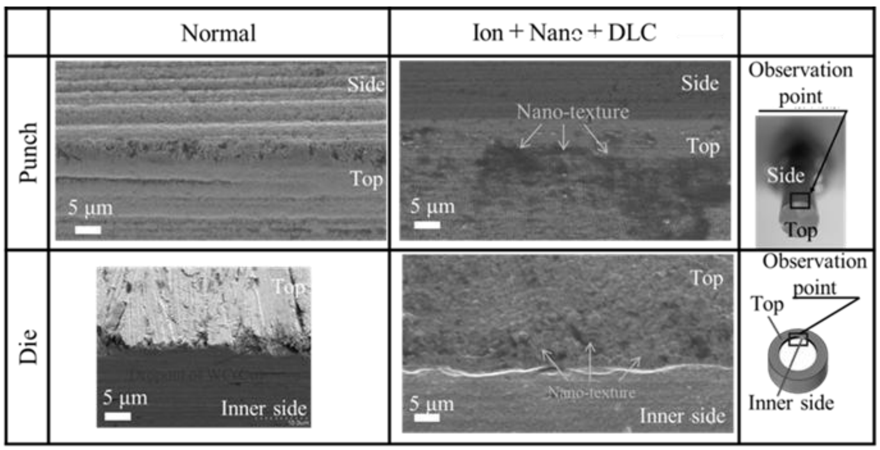

Figure1: Punch and die SEM observation results

3 Experimental results

Figure 2 shows the load–stroke diagrams obtained during punching using the Normal ground tool and the Ion+Nano+DLC treated tool. The horizontal axis represents the stroke [mm], and the vertical axis represents the load [N]. For the normal ground punch shown in Figure 2(a), the maximum load reached 440 N. In the Ion+Nano+DLC condition with a clearance (CL) of 5 μm in Figure 2(b), the maximum load increased to 535 N. In addition, the load increased sharply at 0.188 mm stroke, and then dropped almost vertically, indicating that fracture propagation occurred instantaneously without requiring further stroke. In the Ion+Nano+DLC condition with CL = 2 μm shown in Figure 2(c), the maximum load was reached to 452 N. At a stroke position of 0.065 mm, the load increased sharply to fracture without additional stroke, followed by a sudden load drop. In the Ion+Nano+DLC condition with CL = 1 μm shown in Figure 2(d), the maximum load reached to 525 N. In this case as well, the load increased almost vertically at a stroke of 0.103 mm, and after fracture the load decreased sharply, again indicating instantaneous fracture propagation without additional stroke.

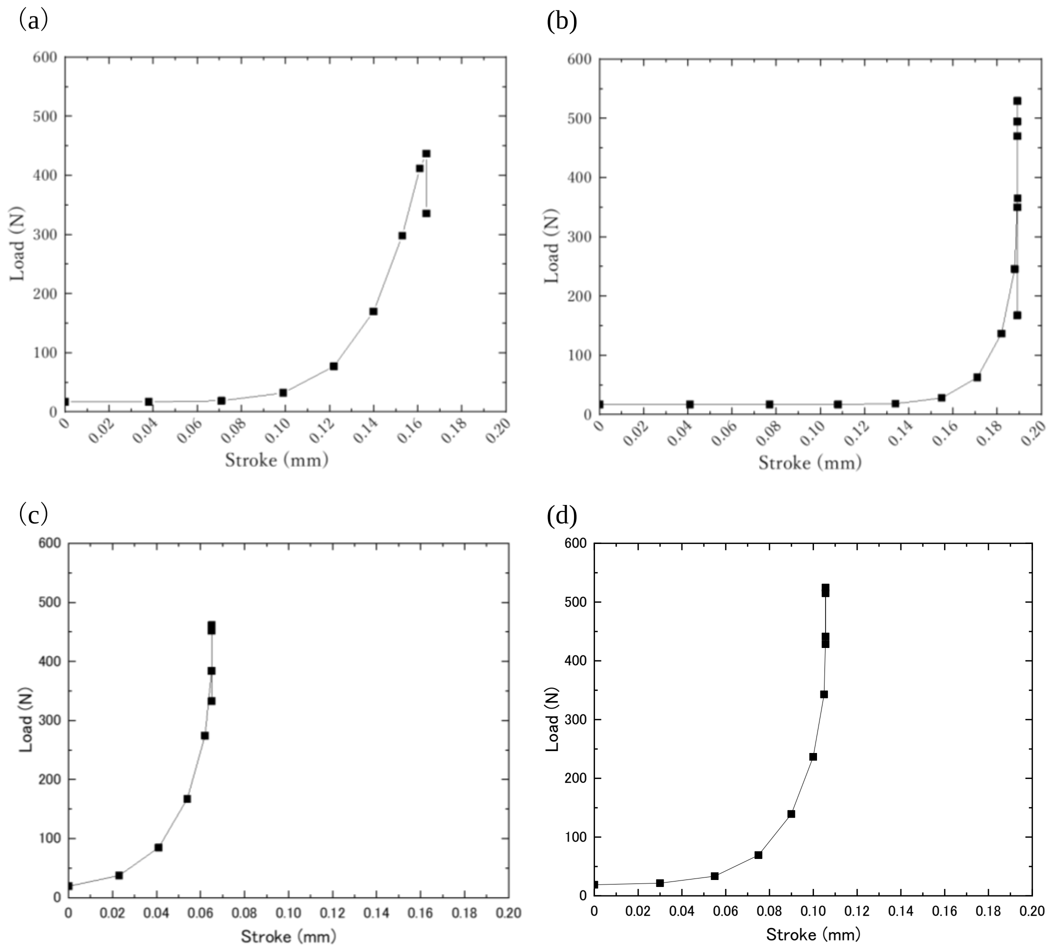

Figure 2: Load-stroke curve of two punch conditions. (a) Normal ground CL 5 μm. (b) Ion+Nano+DLC CL 5 μm. (c) Ion+Nano+DLC CL 2 μm. (d) Ion+Nano+DLC CL 1 μm.

Figure 3 shows the SEM observations of pierced-hole surface and measured crack widths for four punch conditions. Under the normal ground punch condition with CL = 6 μm, cracks are observed at all four-observation side from Left to Front. The maximum crack width is 43.4 μm at the Left side, which exceeds the sheet thickness of 25 μm. The minimum value is 16.2 μm at the Back side, which is still more than three times the clearance. Under the condition of Ion + Nano + DLC CL = 5 μm, the maximum crack width is 20.7 μm on the Back side, which is smaller than the plate thickness of 25 μm. No cracks occurred on the left and front side. Under the condition of Ion+Nano+DLC CL = 2 μm, the maximum crack width on the left side is 10.0 μm. When the clearance is reduced by 2 μm from 5 μm under the condition of Ion+Nano+DLC CL = 5 μm, the maximum crack width is halved from 20.7 μm to 10.0 μm. No cracks occurred on the Back and Right side. Finally, under the condition of Ion+Nano+DLC CL = 1 μm, no cracks occurred on the four sides. It was found that cracking could be completely suppressed by further reducing the clearance from 2 μm to 1 μm under the condition of Ion + Nano + DLC CL = 2 μm.

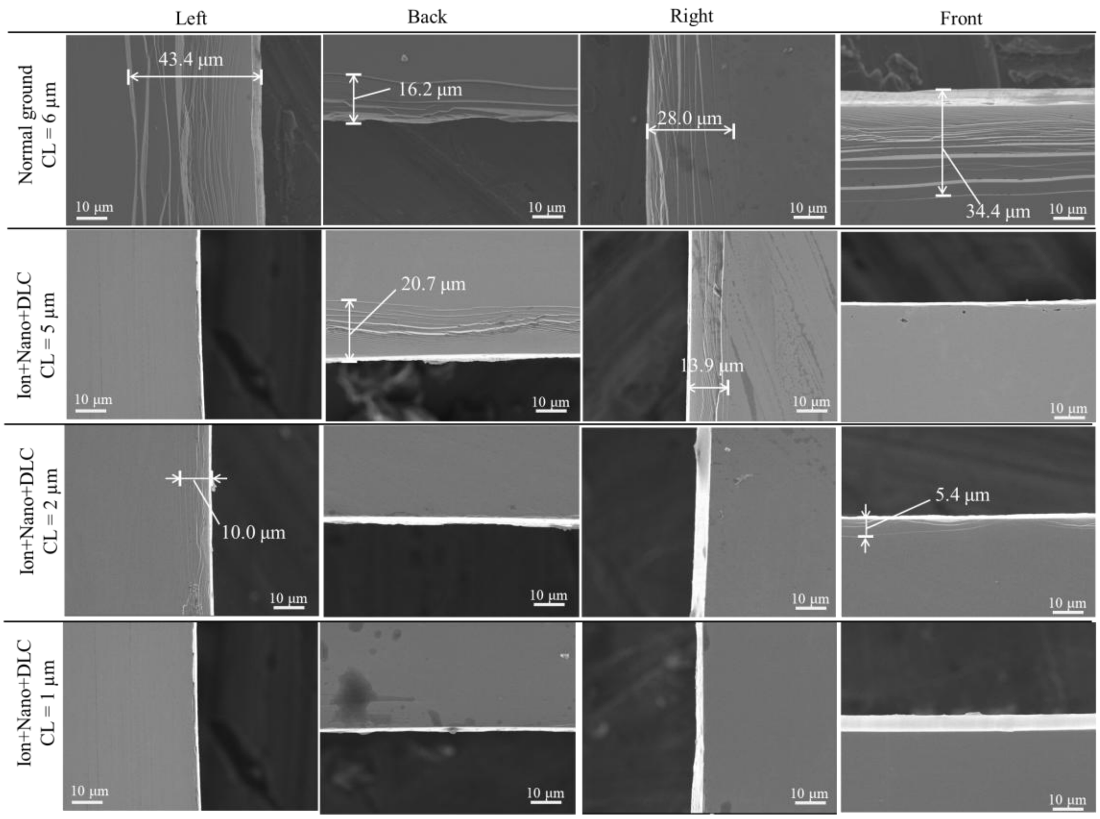

Figure 3: SEM observations of pierced-hole surface and measured crack widths for four punch conditions.

4 Discussion

First, let's consider the punching load and crack initiation in the normal ground condition. From Figure 2 in the normal ground condition, it became clear that the other three conditions, Ion + Nano + DLC, showed a characteristic of fracture before the load rose vertically. Cracks occurred on all four sides of the punched hole. This indicates that, as the workpiece was drawn into the die during the progression of piercing, bending deformation was imposed simultaneously, and cracks were generated predominantly by bending deformation at the workpiece surface. This means that as the workpiece was drawn into the die during the piercing process, bending deformation was applied as it was drawn in, and cracks occurred mainly on the surface of the workpiece due to bending deformation.

As shown in Fig. 3, for the three conditions employing Ion+Nano+DLC, no cracks were observed at two or more of the four observation sides. In addition, Figure 2 indicates that in these three Ion+Nano+DLC conditions the load increased almost vertically. These results suggest that, with using Ion+Nano+DLC, fracture occurred under conditions in which the punching load was concentrated in the stroke direction, leading to yielding and subsequent fracture without the occurrence of cracks caused by bending deformation.

As shown in Figure 1, the edge regions of the Ion+Nano+DLC punch and die are homogeneously sharpened, and a nanometer-scale periodic structure is introduced on this homogenized edge. For the load to increase vertically, the edge portions of the punch and die must be uniform; otherwise, local irregularities cause catching, which results in the workpiece being drawn into the die. In addition, the nanometer-scale grooves of the periodic structure are considered to act like wedges upon contact with the workpiece, thereby firmly gripping the material.

When the clearance was reduced to 1 µm under the three conditions using Ion + Nano + DLC, cracks were suppressed on all four sides. This means that it is necessary to make the clearance as small as possible to prevent the workpiece from being drawn into the die. For amorphous electrical steel sheets with a thickness of 25 µm, even a clearance of 1 µm represents a thickness ratio of 4%. With a clearance of 2 µm, the thickness ratio is reach to 8%, which is the same level as the clearance conditions in general shearing processes. **Figure 4** is a schematic diagram showing the difference in how the workpiece is pulled and drawn in under the conditions of Ion + Nano + DLC 2 µm and Ion + Nano + DLC 1 µm.

It was found that in finishing the punch and die, it is important to create homogeneous tool cutting edge at nanometer scale through ion-sharpening, and to impart a nanometer periodic structure to create a wedge effect and suppress bending deformation on the surface of the punched hole. Reducing the clearance to 1 µm is a factor that maximizes the bending deformation suppression effect of the nanometer periodic structure.

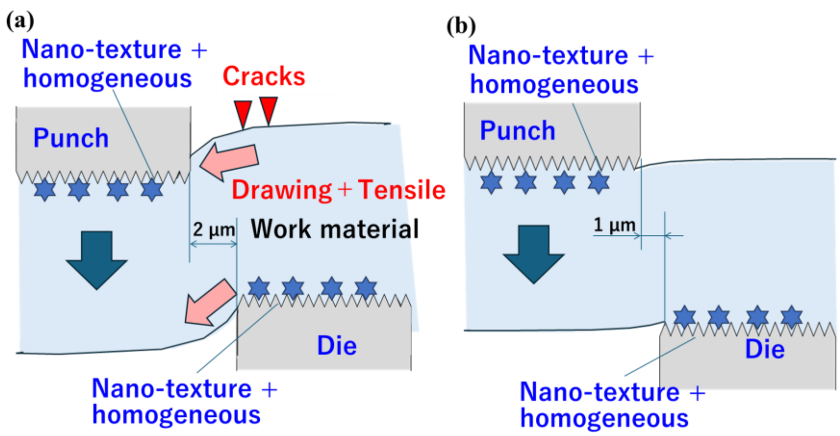

Figure 4: schematic diagram showing the difference in how the workpiece is pulled and drawn in under the conditions of Ion + Nano + DLC CL = 2 µm and Ion + Nano + DLC CL = 1 µm. (a) Ion + Nano + DLC CL = 2 µm condition. (b) Ion + Nano + DLC CL = 1 µm.

5 Conclusion

Experiments were conducted on the shearing of amorphous electrical steel sheets using tools with two different finishes: a normal ground finish and an Ion + Nano + DLC coating, while varying the clearance. As a result, the following conclusions were obtained.

(1) The nanometer-sized homogeneity and nanometer periodic structure of the ion-sharpened tool have the effect of preventing the phenomenon in which the workpiece material is drawn into the die during shearing of amorphous magnetic steel sheets, causing cracks due to bending deformation.
(2) Clearance is an important factor in preventing cracks on the surface of punched holes.
(3) By narrowing the clearance to 1 µm and using an Ion + Nano + DLC tool, it is possible to suppress the occurrence of cracks on the surface of punched holes due to bending deformation.

Acknowledgement

Part of the experiments in this report were supported by a research grant from The Amada Foundation and JSPS KAKENHI. The authors would like to express their sincere gratitude.

References

[1] M. Kimura: "Highly efficient amorphous alloy based motor to mitigate global warming", Proterial technical report, 2023, 38, PP. 38-43.

[2] T. Sato: "Properties and application of amorphous metals", J. Surf. Finish. Soc. Jpn., 1981, 28(11), pp. 556-562.

[3] K. Masumoto: "Properties of amorphous alloys and their applications", J. Japan Inst. Met. Mater., 1984, 23(9), pp. 739-749.

[4] A. Inoue and T. Masumoto: "Recent progress of amorphous alloy", J. Surf. Finish. Soc. Jpn., 1989, 40(3), pp. 361-367.

[5] Y. Enomoto, K. Suzuki, S. Okita, K. Eto, and E. Katayama: "Evaluation of a motor with an amorphous iron core punched by a die", IEEJ Trans. Ind. Appl., 2021 ,10(6), pp. 785–792.

[6] T. Kumagai, H. Sakurai, T. Shioi, H. Kato, J. Itoh, K. Kusaka, T. Yamaguchi, M. Nakagawa, and D. Sato: "Experimental evaluation of a switched reluctance motor fabricated by blanking amorphous alloy foil", J. Surf. Finish. Soc. Jpn., 2022, 11(1), pp. 117–127.

[7] I. Aoki, K. Abe, and T. Nakamura: "Shearing characteristics of amorphous alloy foil", J. JSTP, 1986, 27(306), pp. 860–867.

[8] I. Nakagawa and I. Aoki, : Piercing of amorphous alloy foil" , Bull. J. Met. Soc. Jpn., 1986, 52(3), pp. 409-414.

[9] N. Koga, K. Abe, S. Okada and T. Yamaguchi: "Effects of various blanking conditions on properties of cut surface of amorphous alloy foil and tool life", J. JSTP, 2018, 59(692), pp. 176–180.

[10] I. Aoki, K. Abe, and T. Nakamura: "Tool wear in shearing of amorphous ally foils", J. JSTP, 1986, 27(308), pp. 1078–1083.

[11] Y. Suzuki, K. Abe, T. Aizawa, and T. Shiratori, "Development of piercing punch for high durability and product quality" , J. JSTP, 2023, 64(751), pp. 131-136.

[12] T. Shiratori, T. Yoshino, Y. Suzuki, S. Nakano and M. Yang: "Effects of ion processing of cutting edge of tools on tool wear and punching characteristics in micro punching process" , J. JSTP, 2019, 60(698), pp. 58-63.

[13] R. Okada, K. Ito, T. Funazuka, T. Aizawa and T. Shiratori: "Punch edge topological design for reduction of work hardening damage in shearing of non-oriented electrical steel sheets", Materials, 2024, 18, 568.

[14] T. Akimoto, Y. Kozawa, R. Okada, Y. Suzuki, T. Aizawa and T. Shiratori, "Punch edge topological design for reduction of work hardening damage in shearing of non-oriented electrical steel sheets" , J. JSTP, 2025, 66(777), pp. 188-194.

[15] T. Aizawa, T. Shiratori, Y. Kira, T. Yoshino and Y. Suzuki: "Femtosecond laser trimming with simultaneous nanostructuring to fine piercing punch to electrical amorphous steel sheets" , Micromachines, 2021, 12(5), 568.

[16] T. Shiratori, K. Ito, S. Furuhata and T. Aizawa: "Nano-texturing orientation effect on the piercing behavior of five stacked amorphous electrical steel sheets" , Proc. ESAFORM2024, 2024, pp. 2492-2498.

[17] K. Ito, S. Furuhata, T. Shiratori, Y. Suzuki, and T. Aizawa: "Influence of tool edge geometry on stress distribution state in laminated shearing of amorphous electromagnetic steel sheets", Proc. WCMNM2024, 2024, pp. 34-40.
[18] T. Shiratori, N. Takahashi, S. Furuhata, and T. Aizawa: "Effect punch edge control on crack propagation during piercing of amorphous electrical steel sheets", Proc. ESAFORM2025, 2025, pp. 1013-1019.